A STUDY OF SUPERGRANULATION USING A DIODE ARRAY MAGNETOGRAPH

SIMON P. WORDEN and GEORGE W. SIMON

Sacramento Peak Observatory, Air Force Cambridge Research Laboratories, Sunspot, N.M. 88349, U.S.A.

(Received 7 January, 1976)

Abstract. The evolution of the velocity and magnetic fields associated with supergranulation has been investigated using the Sacramento Peak Observatory Diode Array Magnetograph. The observations consist of time sequences of simultaneous velocity, magnetic field, and chromospheric network measurements. From these data it appears that the supergranular velocity cells may have lifetimes in excess of the accepted value of 24 hours. Magnetic field motions associated with supergranulation were infrequent and seem to be accompanied by changes in the velocity field. More prevalent were the slow dissipation and diffusion of stationary flux points. Vertical velocity fields of 200 m s^{-1} appear to be confined to downflows in magnetic field regions at supergranular boundaries. These downflows are only observed using certain absorption lines. Corresponding upflows in the center of supergranules of less than 50 m s^{-1} may be present but cannot be confirmed.

1. Introduction

Following Leighton *et al.* (1962) the term 'supergranulation' refers only to a horizontal *velocity* phenomenon within the solar photosphere. Any study involving descriptive parameters, such as lifetimes and sizes, must consequently deal with the velocities directly. The development of fast photoelectric magnetographs makes it possible to study the supergranular velocity flow, rather than secondary effects such as the location of chromospheric emission regions. Several questions concerning supergranulation can therefore be investigated.

Supergranulation has been interpreted as a convective flow pattern (Simon and Leighton, 1964; Leighton, 1964, 1969; Simon and Weiss, 1968) and subsequently used in discussions of convective theory. An important parameter in these discussions is the lifetime of the convective 'supergranular cell', since convective theory can provide estimates of the velocity and temperature structure within a convection cell if the lifetime is known. Several studies of supergranular lifetimes have been undertaken. In the statistical studies of Simon and Leighton (1964) and Rogers (1970) the chromospheric emission network as observed in strong absorption lines was used to define supergranular boundaries. Lifetimes close to 24 hr were obtained in this indirect manner. However, detailed studies of magnetic field elements by Smithson (1973) revealed that these elements do not change significantly in their positions over periods of approximately 36 hr. Since magnetic field elements delineate supergranular boundaries (Simon and Leighton, 1964) this observation would lead to supergranular lifetime estimates somewhat longer than 24 hr. Additional evidence for this hypothesis is provided from Livingston and

Solar Physics **46** (1976), 73–91.

Orrall's (1974) observation of long-lived magnetic features with supergranular appearance. These 'cells' had lifetimes of 3–5 days and occurred within active regions.

Smithson (1973) suggested that the shorter lifetime derived from emission network studies was misleading due to the manner in which it was derived; namely, from mathematical cross-correlations. Since the emission network is a 'thin' system defining only cell boundaries, not the entire cell, small changes in the shape of a cell can cause a large decrease in cross-correlation coefficients. This may produce a spuriously short lifetime compared to the real lifetime of the velocity cell. For this reason supergranule lifetimes are more appropriately derived from measurements of the horizontal velocity flow which extend over virtually the entire cell.

Supergranule cell lifetimes are important for another reason. Leighton (1964, 1969) attributed the observed breakup and dispersion over the solar surface of active region magnetic fields to a random-walk process in which the supergranules were responsible for moving the magnetic fields. Earlier studies of supergranule lifetimes by Simon and Leighton (1964) and later by Rogers (1970), derived from cross-correlation studies of chromospheric emission features (such features are thought to be at supergranule boundaries, outlining the supergranule cells), gave lifetime estimates near 20 hr. If supergranules have a mean lifetime near this value then the observed breakup of magnetic active regions can be explained by Leighton's mechanism. Smithson (1973) conducted careful observations of magnetic active regions over a several day span. From these he concluded that motions of individual magnetic points were inconsistent with observed breakup rates for active regions. If the observed magnetic motions are caused by material motions within supergranules, Smithson infers a mean lifetime for supergranules near 40 hr. If this lifetime obtained from magnetic observations is the same as the supergranule velocity cell lifetime then the breakup of active magnetic regions can no longer be attributed to supergranule random-walk processes. In order to determine whether supergranule motions do in fact affect the surface magnetic fields, it is necessary to correlate the magnetic field motions observed by Smithson directly with supergranular velocity observations.

In order to determine mass flow rates within the supergranule, knowledge of the vertical velocity field is needed. Simon and Leighton (1964), Frazier (1970), Deubner (1972), and Musman and Rust (1970) have reported vertical flows associated with supergranulation. However, only the vertical downdrafts associated with magnetic field elements appear well confirmed. A corresponding vertical upflow in cell centers has not yet been shown convincingly. Accurate photoelectric velocity observations are needed to investigate these questions.

This paper reports a time series of observations including simultaneous magnetic, velocity, and emission network information obtained with the Sacramento Peak Observatory Diode Array Magnetograph. The results of this study will be discussed in light of the problems mentioned above. (Part of this work was

presented at the IAU Symposium No. 71, 'Basic Mechanisms of Solar Activity' held at Prague, Czechoslovakia, 24–30 August 1975.)

2. Observations; Description of the Sacramento Peak Observatory Diode Array System and its Calibration

The Sacramento Peak Diode Array system uses the solar image from the vacuum solar telescope. The Array itself consists of 512 diode detectors arranged in linear groups of 32 detectors (Dunn *et al.*, 1974; Rust and Bridges, 1975). Each group can be physically placed in the spectrum at the exit focal plane of the Sacramento Peak Echelle Spectrograph. The image and spectrum are magnified so that each diode detector sees a spatial element of 0.5″, 1.0″, or 2.0″; i.e., effective solar image diameters of 19.6, 9.8, or 4.9 m, respectively. Corresponding spectral resolution ranges from 0.05 Å to 0.25 Å depending on the degree to which the diode detectors are physically masked. Signals from the diode detectors are read and recorded on magnetic tape using the Xerox Data Systems Sigma 3 computer with two-dimensional scanning accomplished by moving the solar image across the spectrograph entrance slit. Each 32 detector group is placed in the core or wings of suitable spectral lines. Those groups in line cores are used to obtain intensity spectroheliograms. Magnetic and velocity measurements are obtained from diode groups situated in opposite wings of absorption lines. Line shifts due to Doppler velocity shifts can be derived from changes in intensity ratios between the detectors in opposite wings of the absorption lines. In a similar manner line shifts of circularly polarized Zeeman components in magnetic regions can be observed. Circular polarization modulation is obtained by passing the light from a magnetically sensitive line through a Potassium di-Deuterium Phosphate (KD*P) electro-optical crystal in conjunction with a linear polaroid filter.

For this study, each observation covered a region 128″ by 128″ on the sun, scanned boustrophedonically in two 64″ by 128″ swaths with a spatial resolution of 1″. Each 1″ square data point consisted of four readings of the 512 diode detectors, two readings for each polarization state of the KD*P modulator. The resulting velocity, magnetic field, and spectroheliogram data were processed on the XDS Sigma 5 computer with programs for calibration and reduction written by C. A. Bridges, A. D. Ruff and G. W. Simon. Scanning time for each observation was 48 seconds.

The diode array configuration for a large portion of the data consisted of eight 64-diode groups, one group placed in each wing of the Fe I 8468 Å line, one group each in the core of Hα 6563 Å, the core of Ca II 8542 Å, the continuum at 6521 Å, and the core and both wings of the He I 10 830 Å line. A single data recording with the solar image held fixed thus covered a line of 64″ on the Sun. The Fe I 8468 Å line, a Zeeman triplet with a Lande factor of $g = 2.5$ was used for the magnetic and velocity observations. The remaining diode groups produced spectroheliograms, from which the location of the chromospheric emission

network was obtained. The Ca II 8542 Å line proved to be most useful for this purpose.

The strongly magnetically sensitive line Fe I 8468 Å presented problems in observing velocities in magnetic regions (cf. Frazier, 1974). Recent observations of magnetic field strengths by Harvey and Hall (1974) in the infrared indicate solar magnetic fields may be as strong as 2000 G in quiet sun locations corresponding to the chromospheric emission network. At such high field strengths the Zeeman splitting of the λ 8468 line becomes so large that the components are completely separated. This complicates the velocity and magnetic field observations. (See the appendix for a more detailed discussion of this problem.) Since important velocity flows exist within magnetic regions, particularly the vertical downflows at supergranular vertices (Frazier, 1970), a velocity measurement free from magnetic field effects is highly desirable. Such velocities can be obtained from Doppler shifts of lines without Zeeman splitting. A list of suitable lines has been published by Sistla and Harvey (1970). The diode setup was altered to include three of these lines in addition to the $g = 2.5$ line λ 8468. Further, these $g = 0$ lines were chosen to represent a range of heights of formation within the solar atmosphere. By using Fe I 4065 Å to represent velocities in the lower photosphere, Fe I 5123 Å to represent an intermediate height, and Fe I 5434 Å to represent the higher atmosphere, about 100–200 km height discrimination is provided (Altrock *et al.*, 1975). Table I lists height of formation data for these lines.

TABLE I
Data for non-magnetic lines used in the vertical velocity investigation

Line	Range of formation heights for wings of the line at disk center $\mu = 1.0$ (Altrock *et al.*, 1975)
Fe I 5123.7 Å	−0 to +310 km
Fe I 5434.4 Å	+90 to +330 km
Fe I 4065.4 Å	−10 to +210 km

The calibration of the diode system is done using a series of plane-parallel glass plates located ahead of the diode detectors. These plates are tilted under computer control to produce artificially a wavelength shift as seen by the diodes. The solar image is placed out of focus to produce a solar spectrum free from wavelength shifts due to solar surface structure. The intensities for each of the 32 (or 64) diode pairs in the blue and red wings of the lines used for velocity study, I_B and I_R, are recorded for 128 known wavelength shifts $\Delta\lambda$ which include the profile and nearby continuum. The resulting I_B/I_R ratio versus $\Delta\lambda$ is fit with a least squares curve for each diode pair. Ratios, rather than the differences, $I_B - I_R$, are used since they are less sensitive to changing light levels. These calibration

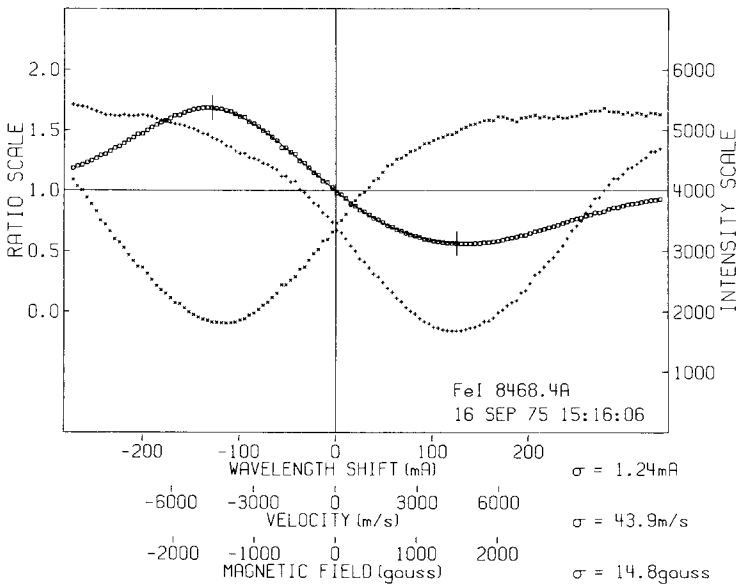

Fig. 1. A typical calibration curve in Fe I λ 8468. Profile seen by diode in blue wing of line (+), by diode in red wing (×), the ratio of the two (□), and the least square fit to this ratio (the solid line between the two vertical bars). Along the abscissa are shown wavelength shifts in units of mÅ, m s^{-1}, and Gauss.

curves are then used to convert observed I_B/I_R values to wavelength shifts $\Delta\lambda$, which in turn are expressed as velocities or magnetic field strengths through the Doppler and Zeeman relations. Basic to this calibration technique is the assumption that the line profile of each point equals that of the average light in the solar region observed. This assumption may lead to significant errors as discussed in the Appendix. The accuracy of this method is limited in part by the accuracies of the I_B/I_R vs $\Delta\lambda$ fits, which typically have standard deviations of 20–40 m s^{-1} over a velocity range ±5 km s^{-1}, and 10–15 G over a range ±1400 G.

An example of a calibration curve is shown in Figure 1. The least squares fit extends from the maximum (R_{max}) to the minimum (R_{min}) of the ratio curve (beyond these limits the ratio function $R(\Delta\lambda)$ is double valued), and is of the form

$$\Delta\lambda(R) = C_0 + C_1R + C_2R^2 + C_3R^3 + C_4R^4 + C_5R^5 + \frac{C_6}{R-R_1} + \frac{C_7}{(R-R_1)^2} + \frac{C_8}{R-R_2} + \frac{C_9}{(R-R_2)^2}$$

in which R_1 and R_2 are approximately R_{max} and R_{min}, respectively. The first six polynomial terms fit the data well for small $\Delta\lambda$, while the last four terms with singular points at R_1 and R_2 are necessary at large $\Delta\lambda$, near R_{min} and R_{max}, where the slope $d(\Delta\lambda)/dR$ becomes infinite.

The tilting plates were also used to correct for spectrograph drift during the course of the observations. The tilt of the plates was adjusted after each

observation so that the net $\Delta\lambda$ for all of the diodes, averaged over all 16 384 data points of the just-completed $128'' \times 128''$ raster remained approximately at zero.

3. Analysis Procedure

Leighton *et al.* (1962) reported a vertical oscillatory velocity in the photosphere with a period about 300 s and with an amplitude of approximately 0.5 km s^{-1}. This phenomenon is of similar velocity amplitude to the supergranular field. As it constitutes an interference to direct observation of the non-oscillatory flow pattern of supergranules it is necessary to remove the 300 s oscillations from these observations. This was accomplished by averaging together the signals from a sequence of individual scans (each taking 48 s of time) over one or more 300 s periods.

The digital nature of the data made it possible to use two-dimensional Fourier analysis by applying a Fast Fourier Transform (FFT) computer algorithm. Since Fourier transforms have the property of separating in frequency-space information on differing size scales they are ideal for supergranular studies. The various velocity phenomena (granulation, supergranulation, and 300 s oscillations) have different spatial scales so the information on each of these velocity fields can be separated within the spatial frequency domain of the Fourier transform. Thus, to isolate supergranular effects the data are transformed and all frequencies representing size scales significantly different than supergranular scales (30 000 km) are removed; then the transform is inverted to produce a filtered picture. However, these filtered pictures obviously suffer from the disadvantage that small scale effects which are associated with supergranulation, such as the downflows at cell boundaries, may also be removed.

Using Fourier analysis in conjunction with conventional means of analysis, such as cinematography of the time sequences obtained, we have studied the lifetime of the supergranular velocity flow, the transport of magnetic field, and the vertical velocity structure of the supergranule.

4. Results

4.1. The lifetime of supergranulation

Several sequences of observations were made, each lasting roughly 10 hours on a single region. While this time was less than the presumed lifetimes (20–40 hr), changes in some supergranules within the observed area may be expected. The data were obtained on 5, 11, and 16 March, 20 April, and 16 July 1974. The data from 5 March, covering 605 min at radius vector $\rho = 0.6$, with consistently good seeing during the entire run, were chosen for detailed analysis.

A movie was made from the original data. The only processing in addition to magnetic and velocity reductions involved time averaging to remove the 300 s oscillation effects. Each frame in the movie consisted of one 288 s average of six

48 s observations. The movie gives the impression that few changes occurred in the supergranular flow pattern during the 10-hr observation period. However, granular velocities were strong and interfered with the definition of supergranular cells. Additionally, when the seeing became more variable, as in the late afternoon, leakage of the 300 s oscillation was present due to inconsistent seeing during the 288 s average. These problems were reduced using the two-dimensional Fourier filtering scheme described earlier, to remove both granulation and the oscillatory leakage. Figure 2 shows samples from the unfiltered data and corresponding filtered images. Each frame consists of an average of 24 observations over roughly four 300 s oscillation periods. Averages over periods longer than 20 min were impractical due to imperfect guiding in the telescope.

From the time sequence in Figure 2, the impression of minimal change in the supergranular pattern, previously noted in the movies, is strengthened. Over the 9 hr period shown in Figure 2, a significant change can be observed in only one of the approximately 9 supergranules present. In the early frames the supergranular flow in the right central part of the picture appears weak; however, later in the day the flow has strengthened. Similar behavior was observed in the data of 11

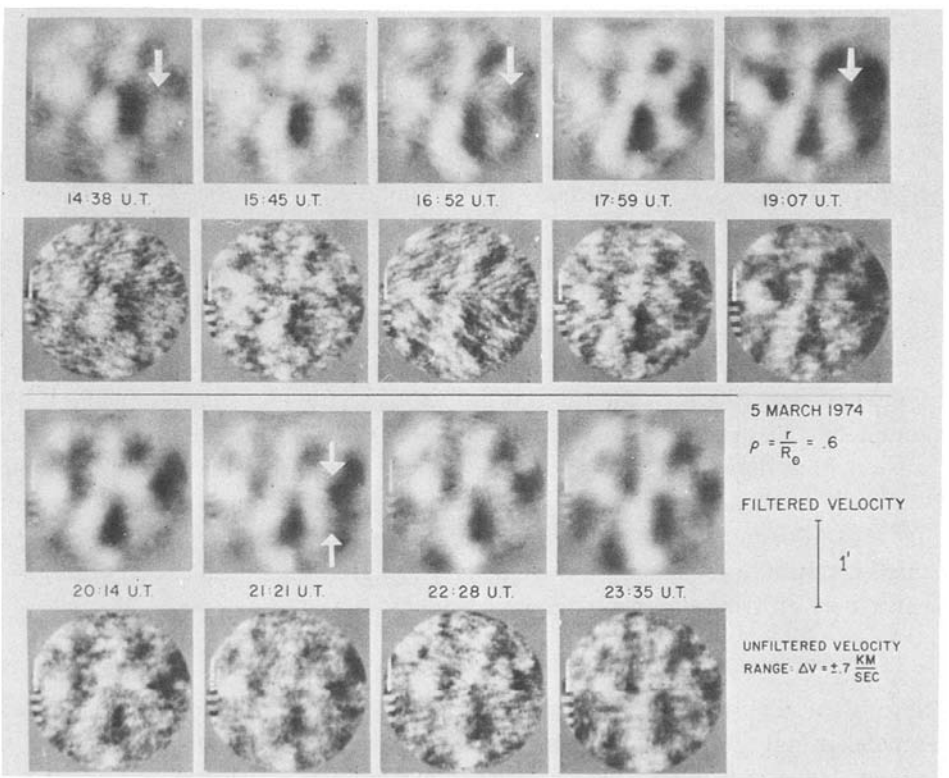

Fig. 2. All day filtered and unfiltered velocity observations for 5 March 1974. Possible changes in the supergranular flow are occurring the marked region.

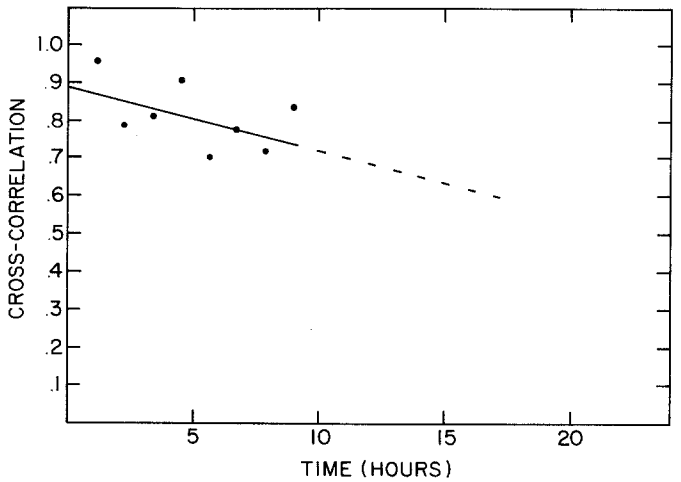

Fig. 3. Cross-correlation in time for the velocity observations in Figure 2.

March and 16 March; again, only 1–2 supergranules in the region under observation appeared to change significantly in the course of the day's observations. Such relatively infrequent changes appear inconsistent with a mean lifetime of approximately 24 hr. If the lifetimes were that short, roughly $\frac{1}{3}$, perhaps 3 or 4 supergranules per day, could be expected to change dramatically in an area covering 9–10 supergranules.

We can derive the lifetime of the supergranular flow from the two-dimensional cross-correlation function, as discussed by Simon and Leighton (1964). The mean lifetime is defined as the time needed for the cross-correlation function to fall to $1/e$ of its original value. The two-dimensional FFT program was used to calculate these functions for the velocity data of 5 March shown in Figure 2. The results are shown in Figure 3. These are independent of signals due to granular velocity structure, since the first data for which cross-correlations were computed are separated by 1 hr in time, during which the granular pattern should have completely changed. The correlation fell to 0.7 of its maximum after 9 hr. A least squares fit to the points shown in Figure 3 gives a slope of 0.017 ± 0.009 yielding a tentative mean lifetime of 36^{+70}_{-12} hr. (The quoted error is one standard deviation.) To verify this longer lifetime, data covering several days are required. However, these results already suggest that velocity cells have lifetimes in excess of the 24 hr value derived from emissions network studies.

4.2. Horizontal Transport of Magnetic Field Associated with Supergranulation

Several of the longer data runs showed evidence of motions of regions with enhanced magnetic fields. Just as for the velocity data, casual inspection of the movies leaves the impression of relative inactivity; however, an occasional horizontal motion of magnetic flux points occurred. As with Smithson's (1973) observations these motions were of several forms. The most frequent form of

motion appeared to be a slow (<1 km s^{-1}) motion of existing flux points in which part of the relatively stationary flux point splits off from the main element and moves away. Figure 4 shows an example of this phenomenon. In most cases the moving flux element moved less than 5000 km and then dissipated. In a few cases of larger velocity (0.5 km s^{-1} $< v <$ 1 km s^{-1}) the daughter flux point moved 5000–10 000 km and remained visible for the remainder of the day.

A more dramatic form of magnetic field motion was associated with the emergence of new flux. In the few cases of this behavior, new flux emerged and moved rapidly (1–2 km s^{-1}) for a distance of 5000–10 000 km. In the three single-day observations available only one or two such events occurred. Additionally, they always appeared in regions where changes in the velocity flow were underway. One such example is present in the data of 5 March. As mentioned

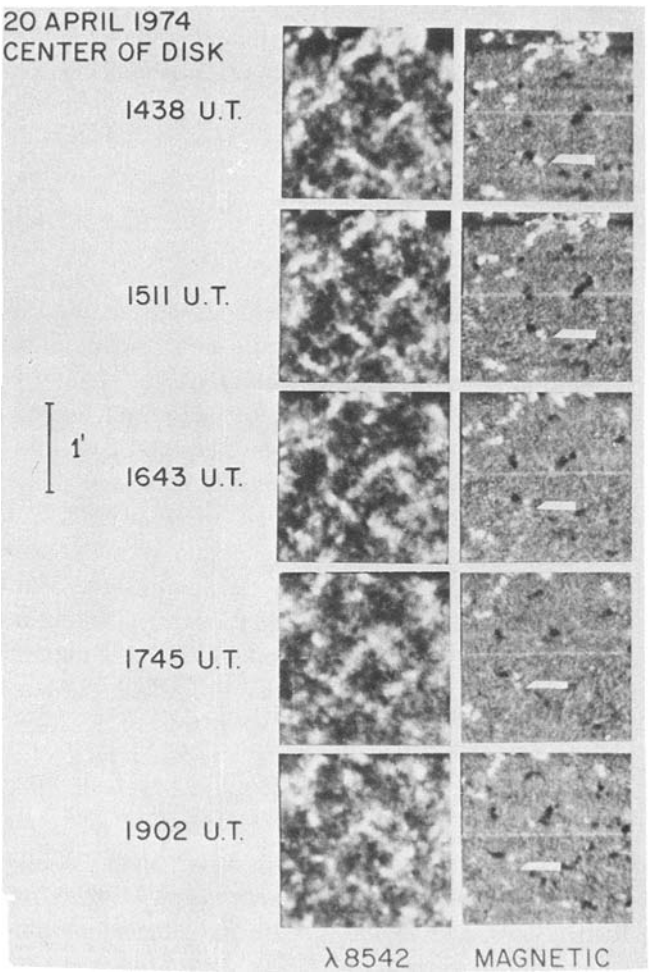

Fig. 4. Example of slow form of flux motion: splitting of existing flux.

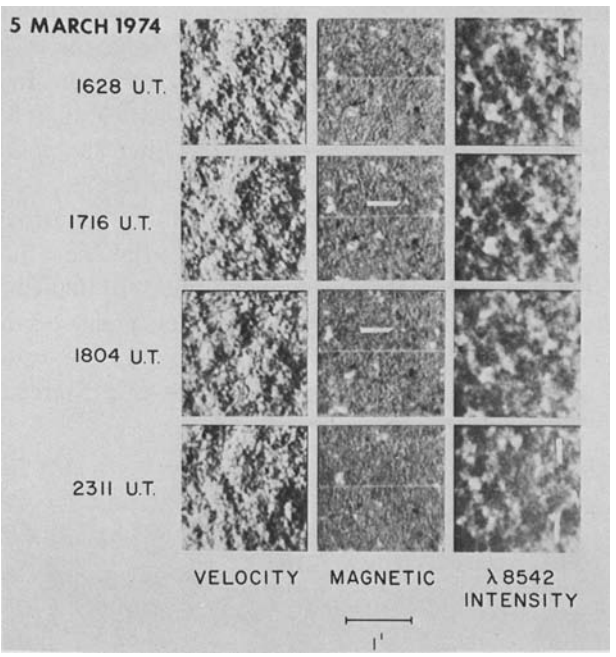

Fig. 5. Example of fast form of flux motion: the appearance of new flux.

previously a velocity cell was observed to change during the day in the right central portion of Figure 2. During this period a small flux point appeared in the center of this supergranule and moved with a velocity of about 1 km s^{-1} towards the boundary of the cell. Figure 5 shows this motion. Associated with this phenomenon, changes also occurred in the chromospheric emission network, as seen in the λ 8542 data in Figure 5. Early in the day the emission network in the region where the velocity cell changes appears to be chaotic. Later, when the velocity flow has become better defined, the emission network has arranged itself into a well-defined network 'cell'. During this period the emission network showed rapid and frequent disappearances, motions, and reappearances. Similar behavior was observed in cases of cell development from the data of the other two days. In all three of these cases, the velocity cell which showed progressively stronger radial outflow from its center, may well represent the formation of a new supergranule.

4.3. Vertical velocity flow within the supergranule

Vertical velocities within supergranules have been reported by several investigators. Simon and Leighton (1964), Tanenbaum *et al.* (1969), Deubner (1972a), Musman and Rust (1970), and Frazier (1970) have detected what appear to be downdrafts at supergranular vertices. However, since Frazier (1970) was only able to observe these downdrafts in certain lines there exists the possibility that the

downdrafts may not be real, but may represent an artifact of the differing line formation, or the magnetic sensitivity of the lines used in the magnetic field regions (Frazier, 1974). Since the observed downflows occur only within the flux elements concentrated at supergranular boundaries this latter suggestion is a distinct possibility. The non-magnetically sensitive lines are ideal for a study of this problem, since they present a range of heights of formation, from levels where magnetic regions differ little in temperature structure from non-magnetic regions to levels where a large temperature differential exists.

The disk center observations of 16 July 1974 were used for this portion of the study. During several hours of the morning during which these data were obtained, the seeing remained excellent (1 to 1.5″). As with the previous data 24 frame averages over 20 min were computed. A resulting 20 min average velocity map for the wavelengths λ 4065, λ 5123, λ 5434, and λ 8468 is shown in Figure 6, together with the filtered images (granular velocities removed), and the simultaneous magnetogram. In the velocity data a large scale pattern, which shows especially well in the filtered images, is apparent. While this pattern appears to have a supergranular size scale, the mean velocity signal is only slightly higher than the noise level. Several methods were used to sort out the true nature of this pattern, which does not appear to correlate well with the magnetic field structure.

To determine whether this pattern is related to the long-lived supergranular flow, observations obtained twenty minutes later during the same run were compared with the earlier data to see if the same velocity structures remained. While a similar large scale velocity pattern was evident, detailed agreement was only partial. Consequently other methods were attempted to study these results.

As mentioned previously, magnetic field elements have been observed to define the vertices of the horizontal supergranule pattern (Simon and Leighton, 1964). A comparison was therefore made between the magnetic field and velocity observations. Only those velocity features which appeared on both consecutive 20 min time averages were used, since supergranular motions should persist over substantially longer periods. Figure 7 shows the result of this procedure, with all velocities less than a threshold of $40\,\mathrm{m\,s^{-1}}$ on both sets of data removed. For comparison the magnetic field structure is also displayed in Figure 7; as expected, the magnetic fields which lie at chromospheric emission locations clearly outline the cellular structure (network) apparent in chromospheric emission data. Upflow of roughly $50\,\mathrm{m\,s^{-1}}$ relative to the reference velocity (the average velocity over the entire frame) appears in the center of some emission network cells. However, downflows in magnetic field regions are apparent *only* in the λ 4065 data. Table II lists the velocities observed for each of the lines as a function of observed magnetic field strength. For small field strength λ 8468 seems to show downdrafts; however, as the field becomes progressively stronger this downflow diminishes in strength, until it disappears entirely. This behavior may be attributable to the magnetic splitting and distortion of this line profile discussed previously.

Two-dimensional autocorrelation functions were used to verify these results. The two-dimensional function can be converted to a one-dimensional function by summing the two-dimensional function over radial annuli. The resulting one-dimensional function is a measure of the correlation of the data field with itself for radial displacements. The mean size scale in the data is given by the half-width of the central autocorrelation peak. Highly periodic data will show secondary maxima at displacements representing the mean size of the periodic structures.

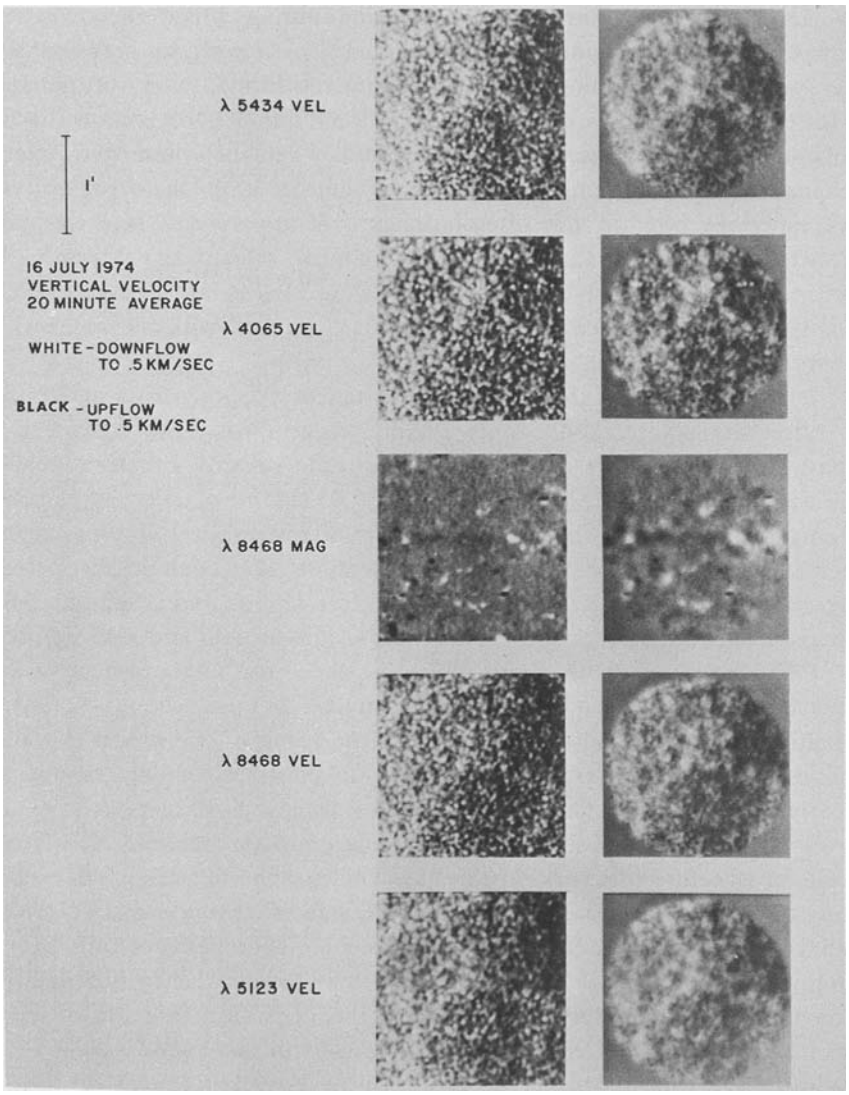

Fig. 6. Filtered and unfiltered velocities in different lines.

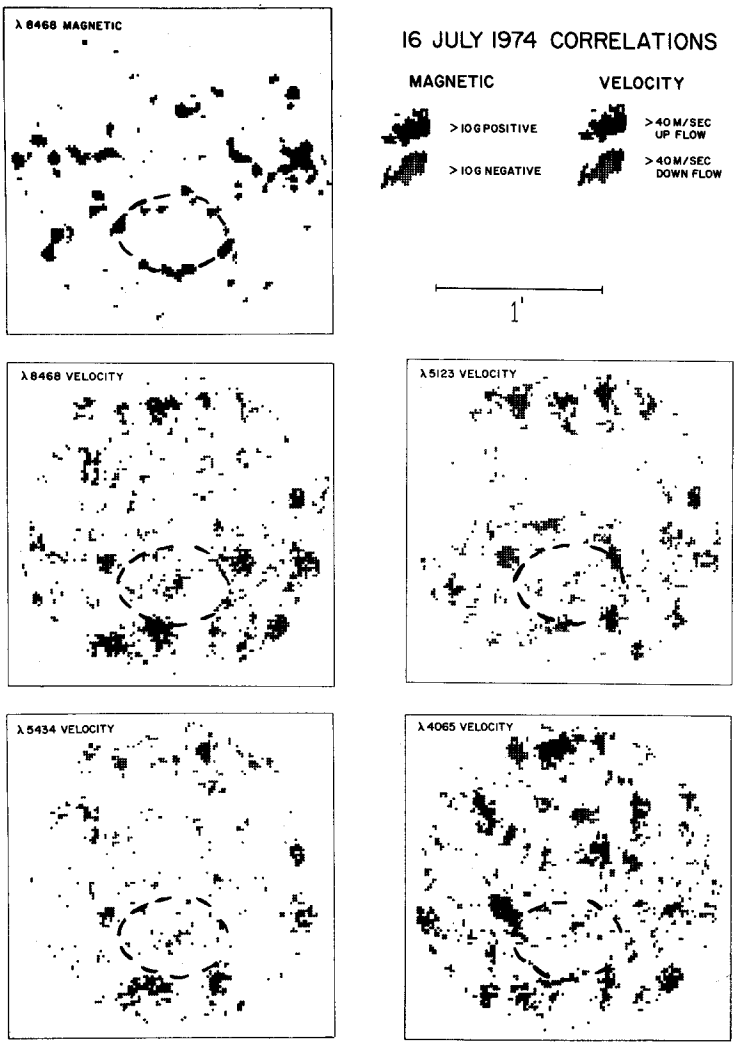

Fig. 7. Velocities and magnetic field above a minimum threshold which correlate over forty minutes in center of the disk data. A network cell has been outlined for comparison.

The radial autocorrelation function summed over 20 min for each of the wavelengths is shown in Figure 8. The sharp fall-offs of the central maxima with full widths at half maximum (FWHM) of 1500 km are probably due to granular signals. However, the more gradual fall-off out to 20 000 km and the possible weak secondary maxima at 30 000 km are indications of vertical velocity structure on a supergranular size scale. The magnetic field autocorrelation function shown in Figure 8 is interesting since its FWHM fall-off of 3500 km is indicative of a mean size of magnetic elements of 4–7″, significantly larger than the seeing size and in line with the visual appearance of the data.

TABLE II

Mean vertical velocities in magnetic field regions (unfiltered data-downflows positive)

Magnetic field threshold	Number of 1″ points used	Velocity ($m\ s^{-1}$)			
		λ 8468	λ 4065	λ 5123	λ 5434
5 G	3140	3±2	14±2	2±1	0±1
10 G	594	13±4	49±4	−3±3	−4±3
15 G	217	15±5	85±7	−16±5	−7±5
20 G	114	13±8.2	105±10	−33±7	−6±6
25 G	67	3±10	116±14	−45±10	−15±8
30 G	39	10±14	153±18	−70±12	−23±8
35 G	28	0±14	174±22	−84±14	−29±10
40 G	19	−9±19	193±26	−92±18	−38±13

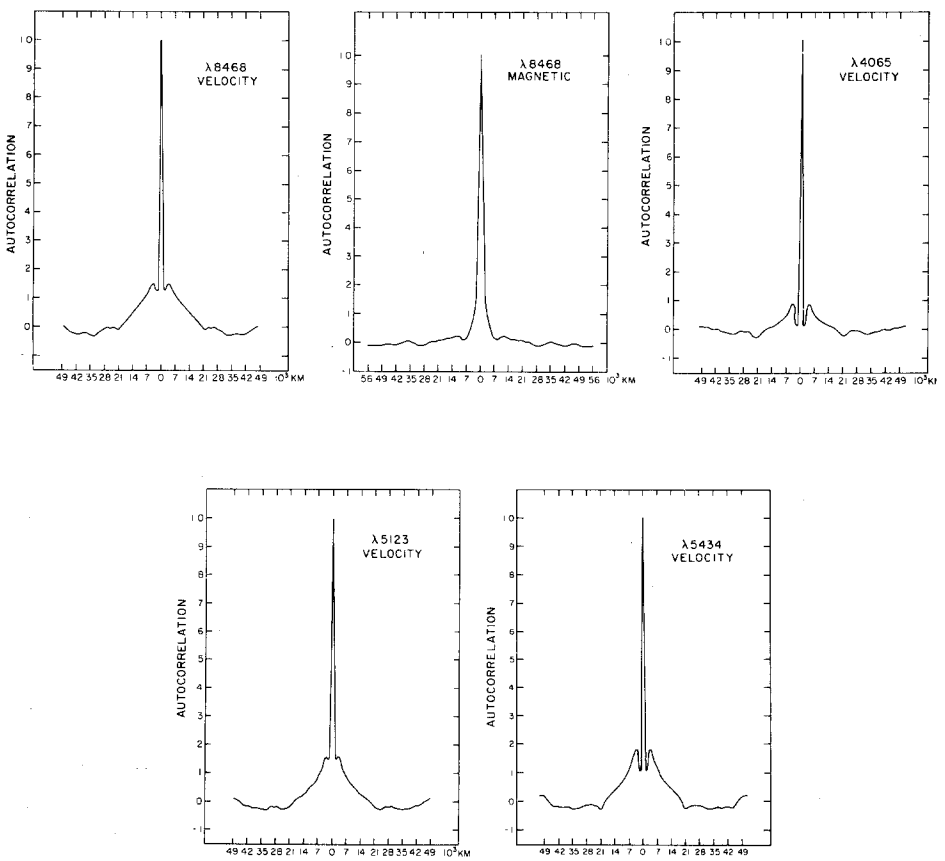

Fig. 8. Radial spatial autocorrelations for the center of the disk data.

5. Summary

We summarize the observational results of this study as follows:

(1) Supergranule velocity cells may have mean lifetimes considerably longer than the previously accepted value of 24 hr, with probable values near 36 hr. However, detailed several-day observations are still needed to verify this lifetime.

(2) No realignments of magnetic field elements already present at supergranular boundaries in a manner expected from Leighton's 'random walk' mechanism were observed in any of the 10 hr runs which were studied. Since 10 hr is only a small fraction of a supergranule lifetime this negative result does not preclude the operation of supergranule random walk processes. However, two forms of magnetic flux motions were observed. Often an existing field element will split and a portion of the flux move away and dissipate. A second form of flux motion occurred when new flux appeared and moved rapidly in regions of changing supergranular flow. The motions are large ($\sim$10 000 km) and rapid ($v \sim 2$ km s^{-1}) in the latter process.

(3) Magnetic field elements have an apparent size of 5″ ($\sim$3500 km) in data with 1 arcsec resolution. This is larger than the seeing size and is presumably real.

(4) Supergranules may exhibit an upflow of $\sim$50 m s^{-1} in the center of the cells; however, this observation needs to be verified with higher accuracy data. A corresponding downflow of $\sim$200 m s^{-1} is observed in magnetic field regions at the boundaries of supergranules. However, this downflow is only observed in the most deeply formed line (λ 4065).

The longer lifetimes of velocity supergranules indicated from this work match Smithson's (1973) values for lifetimes obtained from magnetic field elements. As shown by Smithson this value is too small by a factor of two to explain the observed diffusion of active region magnetic fields as a random walk process due to supergranular motions. The slow breakup of magnetic field elements is difficult to explain in terms of any surface motion. However, this behavior and the sudden emergence of new flux in a supergranule appears more consistent with a model similar to the 'flux-rope' model of Piddington (1975).

Velocity observations are relevant to the general problem of the origin of solar magnetic fields. In models such as Leighton's (1969), convective motions like supergranulation are directly responsible for generating the solar surface magnetic fields through a dynamo mechanism. Conversely, models such as Piddington's (1975) require magnetic fields to be generated deeper than the supergranular convection zone by mechanisms other than the dynamo, with supergranular motions playing almost no role in magnetic field generation. Surface observations, such as those presented here on magnetic fields and velocity fields can provide information on the role which supergranules play in magnetic field generation. While inconclusive, these observations seem to show little direct interaction between magnetic fields and supergranulation, thus supporting Piddington's model. However, it is clear that more definitive information about lifetimes and

other parameters is needed for the large scale surface motions (supergranulation and giant cells). Continuing observations on these motions are currently underway at the Sacramento Peak Observatory.

Acknowledgements

We would like to thank J. W. Harvey, J. M. Beckers, and P. A. Strittmatter for their comments on this work. We also thank F. Hegwer, R. Mann, and H. Mauter for their help with the instrumentation and observations. One of us (S. P. Worden) would like to thank the Kitt Peak National Observatory for support during part of this investigation.

Appendix: Observing Velocities in Magnetic Field Regions

The use of strongly magnetically sensitive lines to observe velocities presents problems (Frazier, 1974). Such lines become so strongly Zeeman split that the circularly polarized components can be separated substantially from the unshifted component. The magnitude of this splitting and the effect on velocity observations can be calculated. If we assume, for the λ 8468 line with $g_{\text{eff}} = 2.5$, a Gaussian line profile, simple Zeeman splitting, with the total magnetic field in the line of sight, the following equation is valid for the splitting of the Zeeman sigma components:

$$\Delta\lambda(\text{Å}) = 4.7 \times 10^{13}\, g_{\text{eff}} \lambda^2(\text{Å})\, \text{H(Gauss)}$$
$$= 8.4 \times 10^{-5}\, \text{Å H(Gauss)}$$

In Table III the field strengths, true velocity magnitude, and the velocity which would be observed using the Zeeman split line are shown. At field strengths larger than a few hundred Gauss, it can be seen that meaningful velocity observations become difficult. Recent observations of magnetic field strength by Harvey and Hall (1974) indicate that quiet sun magnetic fields may be as strong as 2000 G. The lack of any significant velocities in Table II using the line λ 8468 in magnetic regions is thus not surprising. A similar lack of non-zero velocities was also observed in an active region; thus this effect seems well confirmed.

Observations using the non-magnetic lines also showed a systematic effect. As shown in Table II progressively more negative velocities (upflows) are observed with increasing field strength using the λ 5123 and λ 5434 lines. The opposite was the case for λ 4065. Chapman (1974) and Frazier (1974) have suggested that the observed downflow at supergranule vertices may be due to line profile changes in the magnetic field regions caused by heating in the low chromosphere. Since the non-magnetic lines used in part of this study were chosen to represent heights where this effect is important, this hypothesis can be checked. We studied the

TABLE III
Effect of magnetic field on velocity observations with the λ 8468 line

True velocity ($m\ s^{-1}$)	Magnetic field (G)	Observed velocity ($m\ s^{-1}$)
100	0	100
100	200	95
100	400	85
100	600	60
100	800	30
100	1000	5
100	1200	−10
100	1400	−40
100	1600	−45
100	1800	−50
400	0	400
400	200	390
400	400	340
400	600	300
400	800	220
400	1000	60
400	1200	−180
400	1400	−220
400	1600	−260
400	1800	−270
800	0	800
800	200	790
800	400	700
800	600	600
800	800	450
800	1000	200
800	1200	−330
800	1400	−470
800	1600	−520
800	1800	−530

three non-magnetic lines with an LTE computer program developed by R. W. Milkey for the KPNO CDC 6400 computer. The assumed line profiles for these lines are from the *KPNO Preliminary Solar Atlas* (Brault and Testerman, 1973). The profiles were matched using the HSRA model atmosphere (Gingerich *et al.*, 1971). These profiles were then compared to line profiles calculated for the magnetic field (facular) region using a model atmosphere for these regions supplied by Chapman (1970, 1974). The resulting line profiles are shown in Figure 9. As expected, the deeply formed wings are little affected by this change. However, the cores of λ 5123 and λ 5434 are formed in high enough levels so that the facular temperature change is significant. In each case the flat bottom of the profile signifies formation above the temperature minimum. At the least non-LTE conditions hold, the LTE conditions fail, and a greatly flattened core profile is expected for these two lines; also the possibility of a central reversal in

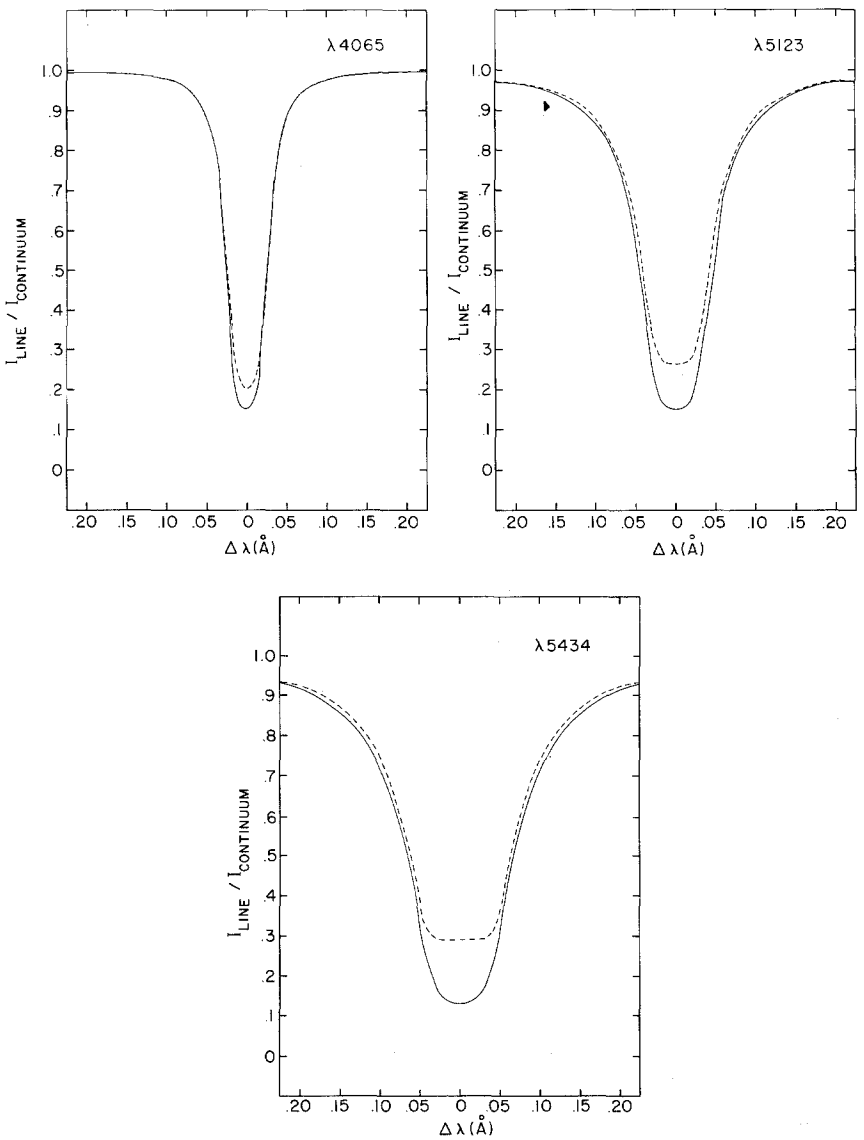

Fig. 9. Line profile calculations for the non-magnetic lines with facular (magnetic field regions) and non-facular atmospheres.

the line is present. Since calibrations were obtained in non-magnetic regions the net effect of this profile change and possible central reversal would be to record substantially smaller velocities than are actually present. The velocities listed in Table II actually appear to become more negative for the λ 5123 and λ 5434 lines with increasing field strength, so it is probable that this effect is present. As the λ 4065 line shows no significant profile changes in the magnetic region it is reasonable to claim it is producing real data concerning velocities present in

magnetic field regions. This leads to the conclusion that the downflows of 200 m s^{-1} observed in these regions are real.

References

Altrock, R., November, L., Simon, G., Milkey, R., and Worden, S. P.: 1975, *Solar Phys.* **43,** 33.
Brault, J. W. and Testerman, L.: 1973, Preliminary Edition of the Kitt Peak Solar Atlas.
Chapman, G. A.: 1970, *Solar Phys.* **14,** 315.
Chapman, G. A.: 1974, private communication.
Deubner, F. L.: 1972, *Solar Phys.* **17,** 6.
Dunn, R. B., Rust, D. M., and Spence, G. E.: 1974, *Proc. SPIE* **44,** 109.
Frazier, E. N.: 1970, *Solar Phys.* **14,** 89.
Frazier, E. N.: 1974, *Solar Phys.* **38,** 69.
Harvey, J. W. and Hall, D. N. B.: 1974, *Bull. Am. Astron. Soc.* **7,** 459.
Leighton, R. B.: 1964, *Astrophys. J.* **140,** 1559.
Leighton, R. B.: 1969, *Astrophys. J.* **156,** 1.
Leighton, R. B., Noyes, R. W., and Simon, G. W.: 1962, *Astrophys. J.* **135,** 474.
Livingston, W. C. and Orrall, F. Q.: 1974, *Solar Phys.* **39,** 301.
Mullan, D. J.: 1971, *Monthly Notices Roy. Astron. Soc.* **154,** 467.
Musman, S. and Rust, D. M.: 1970, *Solar Phys.* **13,** 261.
Piddington, E. H.: 1975, preprint.
Rogers, E. H.: 1970, *Solar Phys.* **13,** 57.
Rust, D. M. and Bridges, C. A. III: 1975, *Solar Phys.* **43,** 129.
Simon, G. W. and Leighton, R. B., 1964, *Astrophys. J.* **140,** 1120.
Simon, G. W. and Weiss, N. O.: 1968, *Z. Astrophys.* **69,** 435.
Smithson, R. C.: 1973, *Solar Phys.* **29,** 365.
Tanenbaum, A. S., Wilcox, J. M., Frazier, E. N., and Howard, R.: 1969, *Solar Phys.* **9,** 328.
Wilson, P. R.: 1972, *Solar Phys.* **27,** 363.